ChemBioChem

Research Article
doi.org/10.1002/cbic.202200512

Chemistry Europe
European Chemical Societies Publishing

www.chembiochem.org

Membrane Permeant Analogs for Independent Cellular Introduction of the Terpene Precursors Isopentenyl- and Dimethylallyl-Pyrophosphate

Francis M. Rossi[+],[a, b] Dillon P. McBee[+],[a] Thomas N. Trybala,[a] Zackary N. Hulsey,[a] Camila Gonzalez Curbelo,[a] William Mazur,[a] and Joshua A. Baccile*[a]

Isopentenyl pyrophosphate (IPP) and dimethylallyl pyrophosphate (DMAPP) are the central five-carbon precursors to all terpenes. Despite their significance, exogenous, independent delivery of IPP and DMAPP to cells is impossible as the negatively charged pyrophosphate makes these molecules membrane impermeant. Herein, we demonstrate a facile method to circumvent this challenge through esterification of the β-phosphate with two self-immolative esters (SIEs) that neutralize the negatively charged pyrophosphate to yield membrane-permeant analogs of IPP and DMAPP. Following cellular incorporation, general esterase activity initiates cleavage of the SIEs, resulting in traceless release of IPP and DMAPP for metabolic utilization. Addition of the synthesized IPP and DMAPP precursor analogs rescued cell growth of glioblastoma (U-87MG) cancer cells concurrently treated with the HMG-CoA reductase inhibitor pitavastatin, which otherwise abrogates cell growth via blocking production of IPP and DMAPP. This work demonstrates a new application of a prodrug strategy to incorporate a metabolic intermediate and promises to enable future interrogation of the distinct biological roles of IPP and DMAPP.

Introduction

Terpenes, a class of biologically derived molecules containing over 80,000 structurally characterized members to date, exhibit an array of activity critical to basic life processes.[1] The biosynthesis of all terpenes originates from the initial condensation of the structurally related building blocks, isopentenyl-pyrophosphate and dimethylallyl-pyrophosphate (IPP and DMAPP, respectively), which in humans are biosynthesized by the mevalonic acid (MVA) pathway (Figure 1A).[2] Levels of IPP and DMAPP are directly involved in cardiovascular disease and are implicated in cancer and neurogenerative disorders such as Alzheimer's disease.[3] In the MVA pathway, DMAPP is biosynthesized from IPP by the action of isopentenyl-pyrophosphate isomerase (IPI).[4] IPP and DMAPP are combined to form farnesyl pyrophosphate, which gives rise to all higher molecular weight terpenes, including cholesterol, dolichol and coenzyme Q.[5] Despite the centrality of IPP and DMAPP in the formation of many biologically important molecules, relatively few strategies have been developed to interrogate their activity.

The negative charge of pyrophosphates at physiological pH makes IPP and DMAPP membrane impermeant, preventing their exogenous addition to biological systems (Figure 1B).[3d] To circumvent this problem, the uncharged, cell permeant alcohol precursors isoprenol (for IPP) and prenol (for DMAPP) have been fed to cells engineered to express non-native kinases, which convert the alcohols into desired pyrophosphates (Figure 1B).[6] This approach is restricted to a limited number of host organisms and is generally targeted toward the enhanced production of a specific terpene rather than a detailed investigation of the independent biochemistry of IPP and DMAPP. An alternate chemical strategy to introduce exogenous IPP and DMAPP into cells is the membrane permanent molecule mevalonolactone (MVA-L), which is hydrolyzed in cells to the IPP precursor mevalonic acid (Figure 1B).[7] As DMAPP is exclusively formed from IPP in the MVA pathway, this approach does not allow for the independent introduction of IPP and DMAPP (Figure 1A, 1B). Hence, a method allowing for exogenous independent addition of precise amounts of IPP and DMAPP that facilitates the detailed interrogation of their metabolism is lacking.

We envisioned that IPP and DMAPP could be made membrane permeant by masking the negative charge on their β-phosphate with esterase-dependent self-immolative esters (SIEs), (Figure 1C). Once inside the cell, hydrolysis of the ester sidechain on the β-phosphate by native general esterase activity would release IPP and DMAPP in a traceless manner (Figure 1C). Herein we report a facile, modular synthesis of cell permeant precursors to IPP (**1a–d**, Scheme 1) and DMAPP (**2a–d**, Scheme 1) and demonstrate that **1a–d** and **2a–d** enter the cell and rescue growth and viability in mammalian cancer cells (U-87MG glioblastoma) treated with pitavastatin (Pita), a statin drug which prevents cell growth through inhibition of MVA biosynthesis (Figure 1A).

[a] *F. M. Rossi,[+] D. P. McBee,[+] T. N. Trybala, Z. N. Hulsey, C. Gonzalez Curbelo, W. Mazur, J. A. Baccile*
Department of Chemistry
University of Tennessee, Knoxville, TN (USA)
E-mail: jbaccile@utk.edu
[b] *F. M. Rossi[+]*
Department of Chemistry
SUNY Cortland, Cortland, NY (USA)
[+] *These authors contributed equally to this work.*

Supporting information for this article is available on the WWW under https://doi.org/10.1002/cbic.202200512

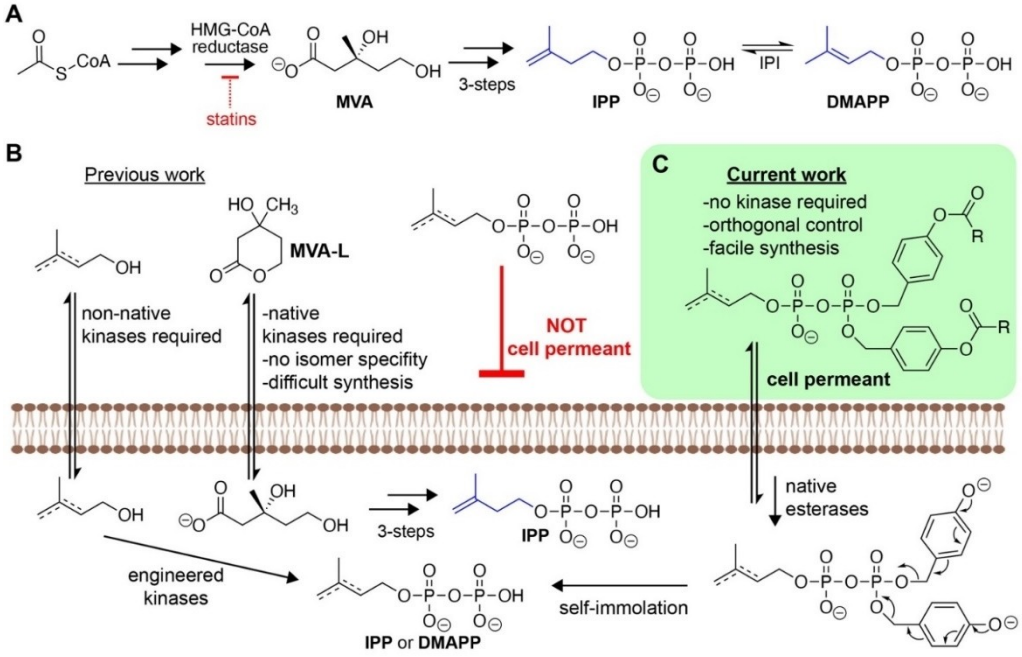

Figure 1. Biosynthesis, cellular permeability and envisioned strategy for making cell permeant analogs of IPP and DMAPP. A) Biosynthetic scheme for IPP and DMAPP starting from acetyl-CoA and proceeding through mevalonic acid (MVA). IPI (isopentenyl pyrophosphate isomerase). B) Isoprenol and prenol are cell permeant but require introduction of non-native kinases to become IPP or DMAPP; MVA-L is membrane permeant but produces both IPP and DMAPP. C) Envisioned strategy for β-phosphate protection to make IPP and DMAPP cell permeant. Once inside the cell, native general esterase activity causes traceless release of IPP or DMAPP.

Results and Discussion

Design and synthesis of cell permeant IPP and DMAPP precursors

Small negatively charged molecules with limited hydrophobicity are typically not membrane permeant. A widely adopted solution to this problem has been to mask the negative charge with esters which, once inside the cell, are cleaved by general esterases to release the negatively charged native compound.[8] While per-esterification of pyrophosphate oxygens impart cell permeability, it also increases the lability of the phosphodiester bond, which causes rapid in-cell pyrophosphate hydrolysis to monophosphates.[9] Meier and coworkers addressed this problem by protecting only the β-phosphate of nucleoside diphosphates with a SIE of *p*-hydroxybenzyl alcohol.[9,10] This self-immolative linker has also been employed for release of a variety of cargos in many biologically relevant applications, such as release of carbonyl sulfide (COS), hydrogen sulfide (H_2S), and lipid nanoparticles.[11]

We hypothesized a similar strategy could be applied to protect the β-phosphate of IPP and DMAPP (Figure 1C). To access the envisioned cell permeant IPP and DMAPP precursors we employed a modular synthetic route (Scheme 1).[9] The required phosphoramidites were prepared as shown in Scheme 1A. Briefly, *p*-hydroxybenzyl alcohol (**3**) was reacted with the appropriate acid chloride to give 4-acyloxybenzyl alcohols **4a–d**. The acid chlorides were selected to provide a range of lipophilicities and ester stabilities to the final IPP and DMAPP analogs. Reaction of 4-acyloxybenzyl alcohols **4a–d** with diisopropylphosphoramidous dichloride gave the desired phosphoramidites **5a–d**. The IPP and DMAPP analogs were synthesized in one pot from the appropriate alcohol and phosphoramidite as shown in Scheme 1B. The monophosphates were first prepared by slow addition of an acetonitrile solution of tetrabutylammonium phosphate to an acetonitrile solution of the alcohol (**6** or **7**, Scheme 1B) and trichloroacetonitrile. Reaction of the resulting monophosphate salt with phosphoramidites **5a–d** and 4,5-dicyanoimidazole, followed by oxidation with *tert*-butyl hydroperoxide gave the desired masked pyrophosphate as the tetrabutylammonium salt. The tetrabutylammonium ion was exchanged for ammonium ion with Dowex 50WX8 resin to give the desired compounds **1a–d** and **2a–d** as ammonium salts suitable for biological evaluation. DMSO solutions of **1a–d** and **2a–d** appear to be stable for months stored in a −80 °C freezer.

Stability of cell permeant DMAPP analogs in cell culture conditions

We sought to confirm the stability of SIE masked compounds under conditions used for mammalian cell culture. Reasoning that our DMAPP analogs (**2a–d**) would be more hydrolytically labile than the IPP analogs (**1a–d**) owing to the DMAPP's ability to form an allylic carbocation, we incubated the DMAPP series **2a–d** in Dulbecco's Modified Eagle Medium (DMEM), pH 7.4, at 37 °C and monitored the disappearance of the phosphate

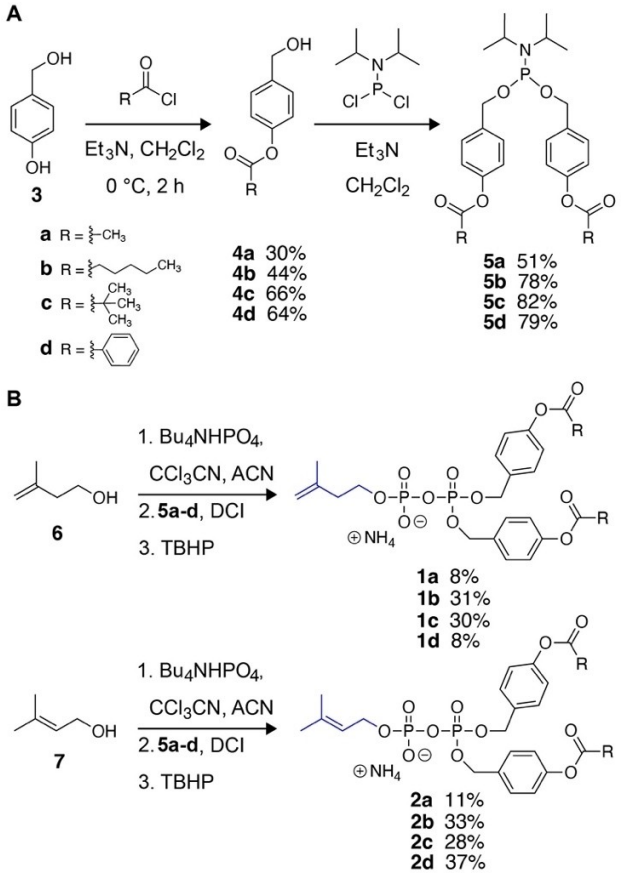

Scheme 1. Modular synthetic approach for accessing cell permeant IPP and DMAPP analogs. A) Synthetic approach for accessing phosphoramidites **5a**–**5d**. B) Conversion of commercially available alcohols (**6** and **7**) to SIE protected IPP and DMAPP in one pot.

diester by liquid chromatography-high resolution mass spectrometry (LC-HRMS, Figure 2A, see Supporting Information for details). Whereas compound **2a** showed substantial degradation over 24 h, compounds **2b**–**d** were relatively stable over the same period. Mammalian cells are typically cultured in the presence of fetal bovine serum (FBS) in order to facilitate cell growth.[3d] To determine if FBS possesses esterases that could prematurely hydrolyze our compounds, we also analyzed the stability of **2a**–**2b** in DMEM with 10% v/v FBS (Figure 2B). The addition of FBS clearly enhanced the degradation of **2a**–**c**, while **2d** was largely unaffected, suggesting that FBS contains esterases that favor sterically unhindered esters. These results show that protection of the β-phosphate is a suitable method for masking the negative charge on DMAPP (and by inference IPP) without compromising hydrolytic stability, so long as the sidechain chosen is sufficiently resistant to spontaneous hydrolysis and hydrolysis by esterases in FBS.

Esterase-dependent release of cell permeant IPP and DMAPP analogs

Once we confirmed the general stability of compounds **2a**–**d** in cell culture conditions, we sought to ensure that they released DMAPP when exposed to an esterase. We treated compounds **2a**–**d** with pig liver esterase (PLE), a promiscuous esterase previously used to evaluate SIE's, and monitored the reaction by LC-HRMS.[12] As expected, we observed ester hydrolysis and subsequent self-immolation of the quinone methide, resulting in the initial release of phosphate monoester and ultimately the release of IPP and DMAPP (Figure 2C and Figure S1). These results further indicate that ester sidechain branching results in differential rates of pyrophosphate release, which could potentially impact bio-utilization of SIE masked IPP and DMAPP.

Rescue of statin inhibited MVA pathway via addition of compounds 1a-2d

With the aqueous stability and esterase-dependent reactivity of the SIE masked pyrophosphates established, we sought to determine if **1a**–**2d** were capable of entering cells and releasing IPP and DMAPP that could be bio-utilized. Previously, Jiang and coworkers showed that treatment of U-87MG cells with statins resulted in cell cycle arrest and loss of cell viability. The normally elongated cells exhibited a rounded morphology, and thus a smaller circumference, when treated with the statin Pita. These effects could be rescued by addition of 100 μM MVA-L, a metabolic precursor to IPP and DMAPP.[3d] We reasoned that if compounds **1a**–**d** and **2a**-**2d** were cell permeant and release their respective pyrophosphates once inside the cell, we would observe a similar rescue phenotype. We treated cells with the statin Pita (10 μM) and **1a**–**d** and **2a**–**2d** (100 μM). MVA-L was used as a positive control and IPP was used as a negative control. Cells imaged over 24 h exhibited a rounding morphology, and thus smaller circumference, when treated with Pita, which was rescued by addition of **1a**–**d** and **2a**–**2d** and the positive control MVA-L (Figure 3, Figure S2 and S3; Supporting Information Movies 1 and 2). Treatment of the same cells with Pita and IPP showed no morphology recovery, confirming that exogenous, unmasked IPP is not bioavailable to U-87MG cells and that the morphological rescue observed in cells treated with **1a**–**d** and **2a**–**2d** resulted from the compounds entering cells. We also evaluated the effects of **1a**–**d** and **2a**–**d** in the absence of Pita. Surprisingly, we observed increased cell circumference with elongated morphology throughout the 24 h incubation for compounds with more stable esters with bulkier side chains (**1c**, **2c**, **1d**, and **2d**) and immediate toxic effects with compounds bearing labile sidechains (Figure S4, Figure S5, and Supporting Information Movie 3). Incubation of cells with the precursor alcohols **4a**–**d** resulted in no observable rescue from Pita treatment (Figure S6).

While morphological recovery of treated cells strongly indicates rescue of the isoprenoid pathway in U-87MG cells, morphology is not necessary directly coupled to viability, a previously shown marker of rescue by MVA-L in statin treated

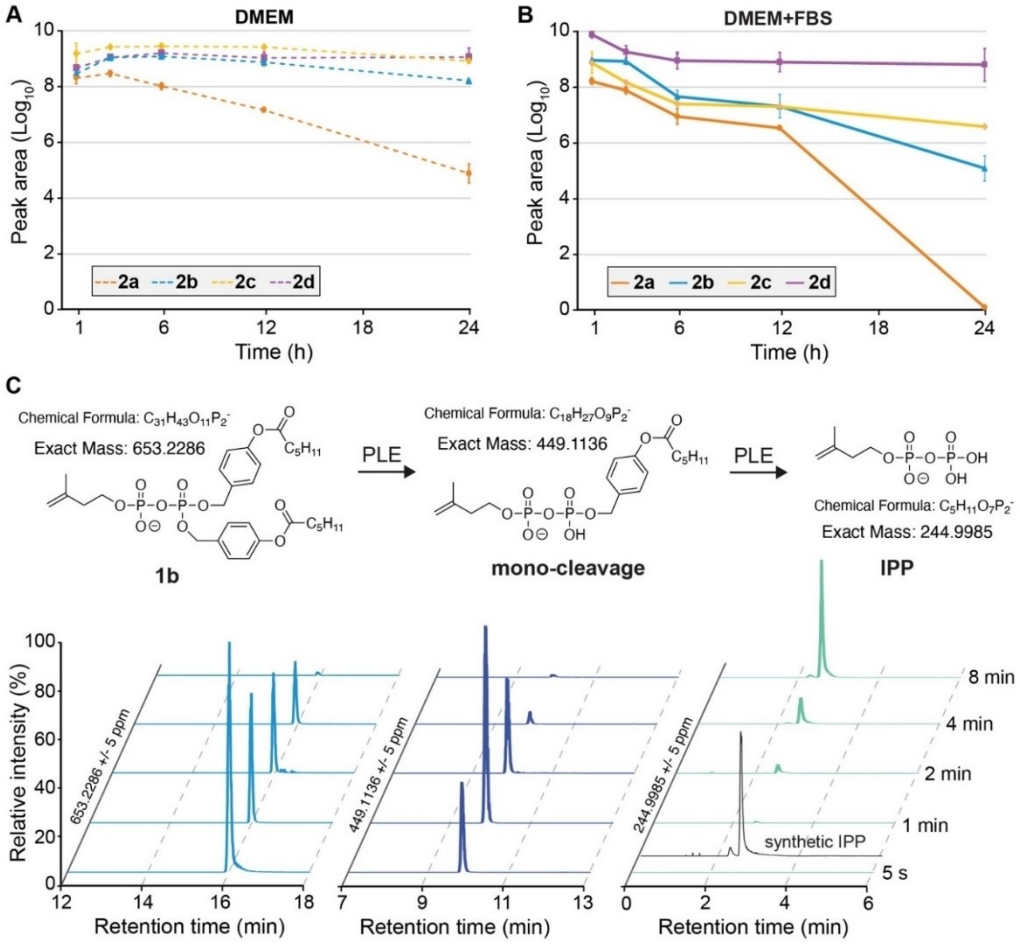

Figure 2. LC-HRMS analysis of stability assays of compounds **2a**–**d**. A) Log_{10} peak area of **2a**–**d** in DMEM, pH 7.4. B) Log_{10} peak area of **2a**–**d** in DMEM with addition of 10% v/v FBS. C) Pig liver esterase (PLE) activity assay of compound **1b** showing extracted-ion-chromatograms (EICs) for **1b** (left, $m/z = 653.2286$), following the first cleavage (middle, $m/z = 449.1136$), and finally releasing free IPP (right, $m/z = 244.9985$), synthetic IPP shown as black line on right.

cancer cells.[3d] To address viability directly, we repeated the feeding experiments with Pita, compounds **1a**–**d** and **2a**–**d**, and measured cell viability after 72 h of incubation following the procedure of Jiang and coworkers.[3d] Similar to the observed rescue in morphology, we saw increased cell viability after 72 h for cells treated with Pita and **1a**–**d** and **2a**–**d**, as compared to cells treated with Pita alone (Figure 4A and 4B). Interestingly, all prepared compounds showed viability rescue after 72 h, whereas, on a shorter timeframe (24 h) we observed morphology recovery in only the subset of compounds with the most durable morphology recovery resulting from treatment with **1c**–**d** or **2c**–**d**. These results indicate that the cellular morphology is a short-term response to the extracellular delivery of IPP and DMAPP; therefore, **1a**–**d** and **2a**–**d** all have sufficient stability and cell penetration to maintain cell viability over longer growth times.

The duration and intensity of morphological rescue appears to correlate well with bulkiness of the ester. Compounds with steric bulk on the ester, pivoyl (**1c** and **2c**), and benzoyl (**1d**, and **2d**), show cell morphology rescue within several hours (Figure 3). The less bulky acetyl (**1a** and **2a**) and hexanoyl derivatives (**1b** and **2b**) have more accessible esters allowing for faster cleavage by native esterases and the rapid release of IPP or DMAPP, which are known to be toxic at high concentrations. The initial reduction in cell size observed during the first six hours of treatment (Figure 3, Figure S2 and S3) is likely caused by either release of the quinone methide by-product or high initial intracellular concentration of IPP or DMAPP, that potentially result in the production of the prenylated ATP derivative, AppppI, a toxic compound know to be produced when levels of IPP are elevated.[13] These results mirror the stability of compounds **1a**–**2d** to general esterases we believe are present in FBS, as LC-HRMS analysis of the supernatants from 24 h incubations with cells show similar trends (Figure S7) and feeding studies conducted with compounds **1a**–**2d** in the absence of Pita (Figure S4). Collectively these results show that the small acetyl ester (**1a** and **2a**) is not ideal for metabolic incorporation experiments, whereas the bulkier esters (**1b**–**d**) and (**2b**–**d**) offer the potential to have distinct release profiles.

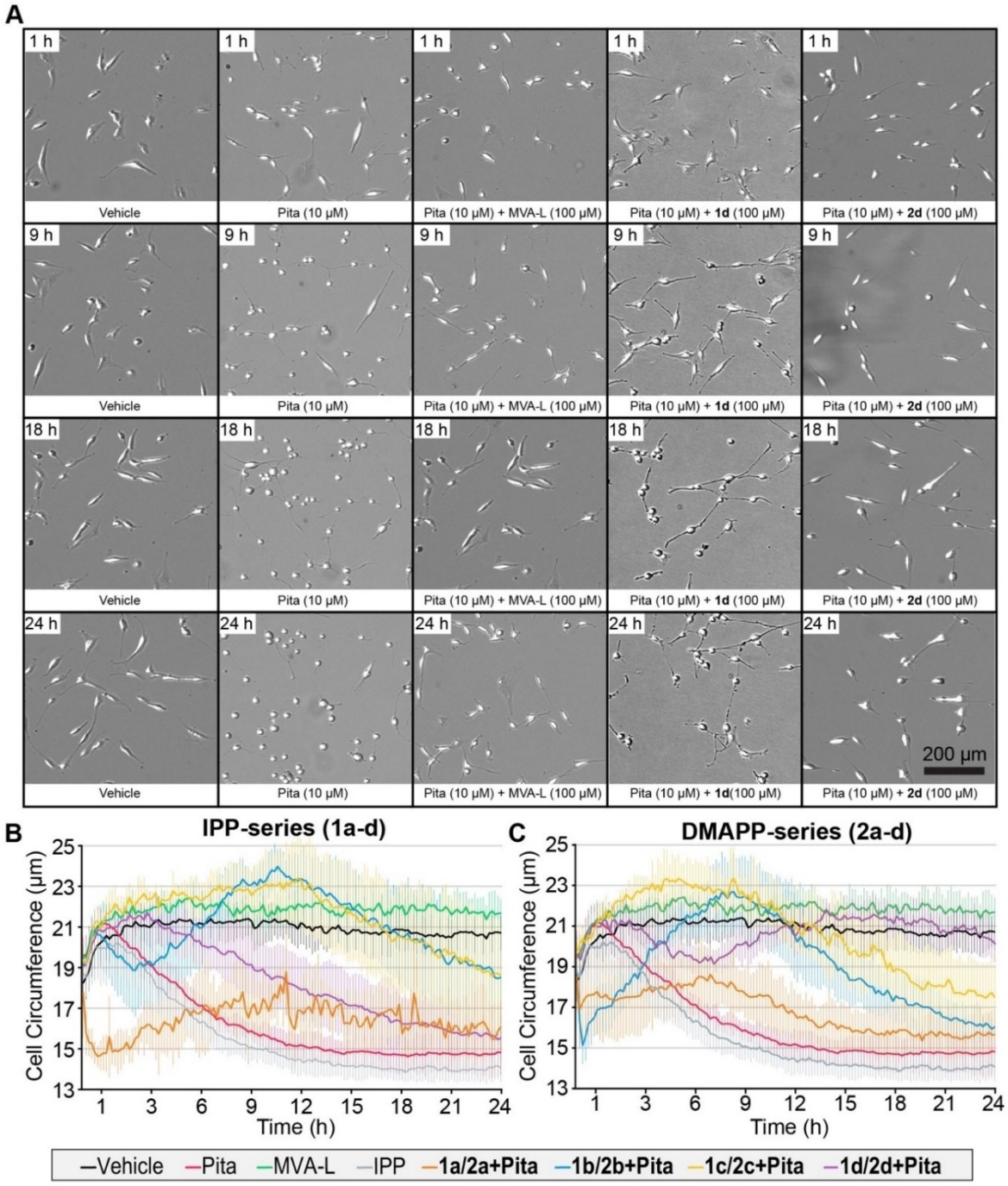

Figure 3. Cell growth assays with U-87MG cells treated with Pita (10 μM) and compounds **1 a**–**2 d** (100 μM). A) U-87 MG cells imaged every 10 min for 24 h, incubated with either untreated Vehicle (DMSO and pluronics, without Pita) or after concurrent treatment with Pita (10 μM) and compounds **1 d** and **2 d** (100 μM). Images were obtained from the Cytation Biotek1 imager with a 4× objective. B) Average cell circumference determined by Gen5 imaging software of U-87MG cells plotted against time after addition of IPP compounds **1 a**–**1 d** (100 μm) with measurements every 10 min for 24 h. C) Average cell circumference determined by Gen5 imaging software of U-87MG cells plotted against time after addition of IPP and DMAPP analogs **1 a**–**2 d** (100 μM) with measurements every 10 min for 24 h.

Conclusion

IPP and DMAPP are central metabolites required to produce a plethora of molecules vitally important in cellular physiology. We show that protection of the β-phosphate on IPP and DMAPP with SIEs imparts cell permeability, subsequent esterase-dependent traceless release and metabolic utilization. Rescue studies of the statin treated U-87MG human cancer cell line show that the sidechain of the self-immolating esters modulates the stability and release rate of IPP and DMAPP. The modular

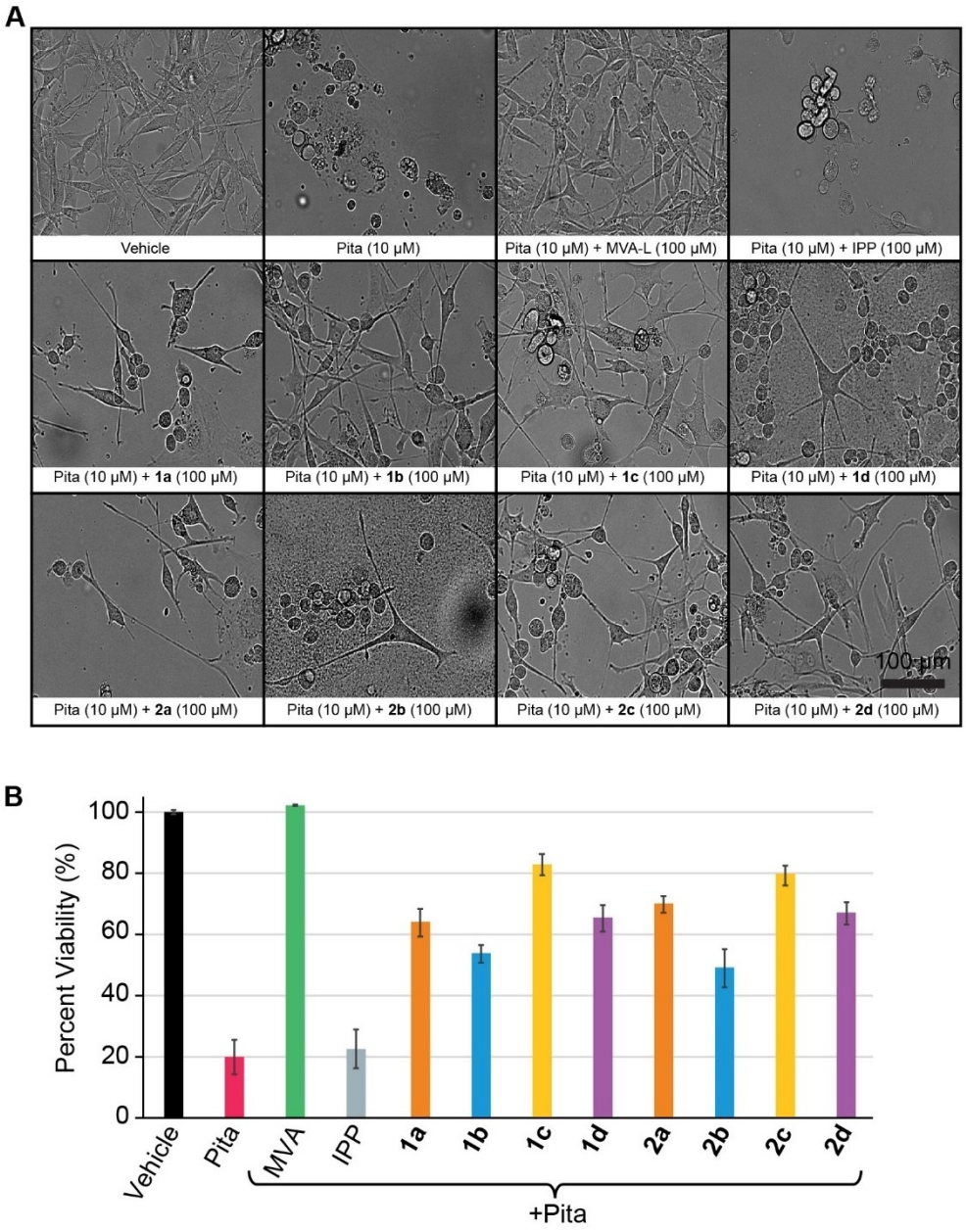

Figure 4. Cell growth and viability assays with U-87MG cells treated with Pita (10 μM) and compounds **1a**–**2d** (100 μM). A) U-87 MG cells imaged 72 h after concurrent treatment with Pita (10 μM) and compounds **1d** and **2d** (100 μM). Images were obtained from the Cytation Biotek1 imager with a 20× objective. B) alamarBlue cell viability assay results for vehicle control, Pita, MVA, IPP, and compounds **1a**–**d** and **2a**–**d** after 72 h incubation. Percentages are relative to vehicle (DMSO plus pluronics), see Supporting Information for more details.

and facile synthetic route reported here enables access to a wide range of SIEs which could potentially be used for targeted release of IPP and DMAPP. The prodrug-like strategy described will enable future isotopic labeling studies of IPP and DMAPP, has the potential to permit interrogation of the independent roles of IPP and DMAPP themselves, is applicable to other membrane impermeant metabolic intermediates, and has potential to be leveraged in other organisms with general esterase activity, such as some fungi and bacteria.

Experimental Section

Synthetic materials: Chemicals were purchased and used without further purification. Where applicable, dry solvents were prepared by freshly distilling and storing over 3 Å molecular sieves. Unless otherwise indicated, all reactions were carried out in oven-dried glassware under an inert atmosphere of argon that was pre-dried by passing through calcium sulfate. Thin-layer chromatography (TLC) was performed using either Baker-flex® disposable TLC plates (J.T. Baker) or TLC Silica gel 60 F_{245} glass-backed TLC plates (Millipore Sigma). Visualization was achieved either using UV light (254 nm) and/or staining in $KMnO_4$ (1.5 g $KMnO_4$, 10 g K_2CO_3, 1.25 mL 10% NaOH in 200 mL of H_2O) and developing with heat.

Flash chromatography of crude products was carried out using a Buchi Pure C-850 FlashPrep chromatography system using pre-packed silica or C18 cartridges where indicated.

NMR spectroscopy: ^{1}H, ^{13}C, and ^{31}P spectra were recorded on a Bruker Ascend 500 (500 MHz) with a Bruker 5 mm BBFO SmartProbe with the indicated solvents used as the internal deuterium lock.

^{1}H,^{13}C, and ^{31}P chemical shifts are reported in δ, relative to the undeuterated residual solvent peak.[14] All spectra are referenced using the residual solvent signal of the indicated solvent. ^{31}P spectra were referenced using absolute referencing to the ^{2}H lock signal in the indicated solvent.

The multiplicity of each signal is indicated by: s (singlet); br s (broad singlet); d (doublet); t (triplet); q (quartet); dd (doublet of doublets); ddd (doublet of doublet doublets); m (multiplet). The number of protons (n) for a given resonance signal is indicated by nH. The coupling constants were determined by analysis using Mestrenova software (version 12.01) and reported to the nearest 0.1 Hz.

Synthetic procedures for compounds 1 a–5 d

General procedure A: synthesis of 4-acyloxy benzyl alcohols: Acid chloride (30 mmol) was added dropwise to a suspension of 4-hydroxybenzyl alcohol (3.72 g, 30 mmol) in triethylamine (4.18 mL, 30 mmol) and dichloromethane (200 mL) cooled on an ice/water bath. After 2.5 hours, the reaction mixture was extracted with water (2×100 mL) and brine (100 mL). The organic layer was dried with anhydrous magnesium sulfate, filtered, and the solvent was evaporated under reduced pressure. Gradient automated flash chromatography of the residue (hexane/ethyl acetate 0–100% over 30 minutes), followed by evaporation of solvent gave the 4-acyloxy benzyl alcohol 4.

General procedure B: synthesis of phosphoramidites: A mixture of acyloxy benzyl alcohol 2 (12.03 mmol) and triethylamine (1.68 mL, 12.03 mmol) in THF (15 mL) was added dropwise over several hours (~1 drop per min) to a solution of diisopropylphosphoramidous dichloride (1.13 g, 5.60 mmol) in THF (20 mL) that was cooled on an ice/water bath. After the addition was complete, the reaction mixture was allowed to come to room temperature and stirred, overnight. The reaction mixture was filtered and the precipitate was rinsed three times with a small amount of hexane. The combined filtrates were evaporated under reduced pressure and the residue was purified using gradient automated flash chromatography on a silica gel column pretreated with 2.5% triethylamine in hexane (isocratic 2.5% triethylamine in hexane (5 min); 2.5% triethylamine in hexane/ethyl acetate 0–10%). Evaporation of solvent gave phosphoramidite 5.

General procedure C: synthesis of pyrophosphates: A solution of tetrabutylammonium phosphate (0.255 g, 0.75 mmol) dissolved in acetonitrile (3 mL) was added dropwise over 10 minutes to a solution of 3-methyl-3-butene-ol or 3-methyl-2-butene-ol (IPP or DMAPP respectively, 2.25 mmol) and trichloroacetonitrile (82.7 μL, 0.825 mmol). After 20 minutes, additional trichloroacetonitrile (0.015 mL, 0.015 mmol) was added and the reaction mixture was stirred for 20 minutes. The solvent was removed under reduced pressure and the residue was placed on the vacuum line overnight to remove residual alcohol. Phosphoramidite 3 (0.90 mmol) was added to the residue and the combined mixture was dissolved in acetonitrile (2.5 mL). 4,5-Dicyanoimidazole (0.25 M in acetonitrile) was added in three portions (1.2 mL each) five minutes apart. The reaction mixture was stirred for three hours. *tert*-Butyl hydroperoxide (~5.5 M in decane, 0.164 mL, 0.90 mmol) was added and the reaction mixture was stirred for one hour. The solvent was evaporated under reduced pressure and the residue was chromatographed using a C18 EcoFlex column (12 g, pre-equilibration with water for 10 min, eluting with water for 10 min, followed by eluting with a water acetonitrile gradient, 0%–100% acetonitrile over 30 min). Fractions containing the product were pooled and lyophilized. The residue was taken up in acetonitrile (~0.5 mL) and ammonium bicarbonate/isopropyl alcohol (~0.5 mL, 25 mM ammonium bicarbonate, 2% isopropyl alcohol) and ion exchanged (Dowex 50WX8, 18 g; washed with water, 30 min; 1 M HCl, 20 min; water, 20 min; 25% ammonium hydroxide, 20 min; and 25 mM ammonium bicarbonate, 2% isopropyl alcohol, 20 min. Elution buffer, 25 mM ammonium bicarbonate, 2% isopropyl alcohol). Fractions containing the product were pooled and lyophilized. The residue was dissolved in water (~0.5 mL) and acetonitrile (~0.5 mL) and chromatographed using a C18 EcoFlex column (4 g, pre-equilibration with water for 10 min, eluting with water for 10 min, followed by eluting with a water acetonitrile gradient, 0%-100% acetonitrile over 30 min). Fractions containing the product were pooled and lyophilized to give pyrophosphate 1 or 2. Compounds **1 a** and **2 a** were purified using an alternate method using preparatory chromatography. The lyophilized pooled fractions collected from ion exchange were instead purified using a PrepPure C18 preparative column (100 Å, 10 μm, 250×30 mm). The column was equilibrated with water for 10 minutes at a flow rate of 30 mL min^{-1} followed by elution with water for 10 minutes followed by eluting with a water acetonitrile gradient, 0%-100% acetonitrile over 30 min.

Liquid-chromatography high-resolution mass spectrometry (LC-HRMS): LC-HRMS analysis was performed using a Thermo Scientific Exploris™ 120 mass spectrometer coupled to a Vanquish UPLC system. Separations were carried out under the following chromatographic conditions using a Luna® Omega Polar C18 column (1.6 μm, 100 Å, 150×2.1 mm) operating at a flow rate of 0.150 mL min^{-1}.

Mobile phase A: 10 mM aqueous ammonium bicarbonate

Mobile phase B: 1 : 1 methanol: acetonitrile

Column temperature (°C): 45

Sample temperature (°C): 4

Injection volume: 2 μL

The gradient was programmed as follows: 100% A for 2 minutes to 100% B over 15 minutes. Hold 0.5 minutes then to 100% A over 0.5 minutes. The mass spectrometer was operated under the following tune and scan parameters:

Positive ion (V): 3400

Negative ion (V): 2000

Sheath gas (arb): 35

Aux gas (arb): 7

Ion transfer tube temp (°C): 320

Vaporizer temp (°C): 275

Orbitrap resolution: 120000

Scan range: 100–1000 m/z

RF Lens (%): 70

Maximum injection time: 100 ms

Microscans: 1

Porcine liver esterase (PLE) activity assay: Compounds **2a**–**2d** were mixed with a 15% w/v pluronics solution in DMSO 1:1 (v:v). This was diluted in PBS to a final concentration of 150 μM and a total volume of 100 μL. PLE was added at a working concentration of 0.308 U/mL. Aliquots (10 μL) were taken at 0, 30, 60, 120, 240, and 480 s and were quenched using 30 μL of methanol followed by flash-freezing in liquid nitrogen. Upon completion of the assay, samples were thawed and sonicated for 5 min, followed by centrifugation at 18,000 g for 18 min. The supernatant was transferred to an autosampler vial and stored at −80 °C until LC-HRMS analysis.

U-87MG cell culture: Uppsala 87 Malignant Glioma (U-87 MG) were obtained from ATCC (Manassas, VA). Cells were grown in Dulbecco's modified eagle medium (Gibco) supplemented with 10% (v:v) fetal bovine serum (Gibco), and 50 U/mL penicillin/streptomycin (Gibco) in a humidified incubator at 37 °C, 5% CO_2.

Cells were plated from 100 mm dishes at 80–90% confluency into 24-well plates at a seeding density of 2×10^5 cells per well. Feeding of the compounds took place after 24 hours of incubation after seeding.

Microscopy and cell morphology analyses: 24-Well plates of U-87 MG were imaged using a bright field 4× objective every 10 min for 24 h using the Cytation 1 cell imaging multimode microplate reader (BioTek Instruments, Winooski, VT). Cell morphology was measured as the average object circumference with a size range of 10 μm and to 100 μm using Gen5 software (BioTek Instruments, Winooski, VT). The object size was averaged between wells of the same compound and plotted as cell circumference vs time. Additionally, cell count and object total area (not shown) were measured using Gen5 software. All measurements of cell size are from six trials on two separate 24-well plates.

Pitavastatin rescue assays with compounds 1a–2d: 24-Well plates of U-87 MG cells at 4×10^4 cells/mL were allowed to grow for 24 h or until fully adhered to the 24 well plate. Freshly prepared pitavastatin was added to each well (1 μL, 10 μM) and compounds **1a**–**2d** were mixed 1:1 (v:v) with 15% pluronics in DMSO and added to the appropriate well (2 μL, 100 μM final concentration). 24-Well plates were placed into the Cytation 1 cell imager at 5% CO_2 and the cells were imaged at the center of each 24-well every 10 min for 24 h.

alamarBlue Viability Assay: A 24 well plate of U-87 MG cells seeded at 4×10^4 cells/mL were grown for 24 h or until fully adhered to the 24-well plate. Freshly prepared pitavastatin was added to each well (1 μL, 10 μM) and compounds **1a**–**2d** were mixed 1:1 (v:v) with 15% pluronics in DMSO and added to the appropriate well (2 μL, 100 μM final concentration). The 24-well plates were incubated for 72 h and imaged using a Cytation 1. alamarBlue™ (100 μL) HS cell viability reagent (Invitrogen) was added to each well and fluorescence at 590 nm was measured. Fluorescence was normalized as a percentage using the flowing formula:

$$\frac{Sample\ 590\ nm}{Vehicle\ 590\ nm}\times 100.$$

All additional synthetic materials, procedures, supporting figures and supporting spectra can be found in the accompanied Supporting Information.

Acknowledgements

This work was supported by the National Science Foundation Chemistry of Life Processes (NSF-CLP) program (CHE-2204170). C.G.C. was supported by an NSF REU Fellowship (CHE-1852160). The authors would like to thank Dr. Joseph P. Y. Kao of the University of Maryland Medical School for useful conversations and Lindsay Brown of the Biological and Small Molecule Mass Spectrometry Core (BSMMSC) at UTK for assistance with LC-HRMS.

Conflict of Interest

The authors declare no conflict of interest.

Data Availability Statement

The data that support the findings of this study are available from the corresponding author upon reasonable request.

Keywords: cell permeability · isopentenyl pyrophosphate and dimethylallyl pyrophosphate · isoprenoids · self-immolative esters · terpene biosynthesis

[1] a) J. D. Rudolf, T. A. Alsup, B. Xu, Z. Li, *Nat. Prod. Rep.* **2021**, *38*, 905–980; b) J. S. Dickschat, *Angew. Chem. Int. Ed.* **2019**, *58*, 15964–15976; *Angew. Chem.* **2019**, *131*, 16110–16123.
[2] a) J. C. Sacchettini, C. D. Poulter, *Science* **1997**, *277*, 1788–1789; b) D. W. Christianson, *Science* **2007**, *316*, 60.
[3] a) J. L. Goldstein, M. S. Brown, *Nature* **1990**, *343*, 425–430; b) A. Jeong, K. F. Suazo, W. G. Wood, M. D. Distefano, L. Li, *Crit. Rev. Biochem. Mol. Biol.* **2018**, *53*, 279–310; c) S. Zahra Bathaie, M. Ashrafi, M. Azizian, F. Tamanoi, *Curr. Mol. Pharmacol.* **2017**, *10*, 77–85; d) P. Jiang, R. Mukthavaram, Y. Chao, N. Nomura, I. Bharati, V. Fogal, S. Pastorino, D. Teng, X. Cong, S. Pingle, *Br. J. Cancer* **2014**, *111*, 1562–1571.
[4] K. Berthelot, Y. Estevez, A. Deffieux, F. Peruch, *Biochimie* **2012**, *94*, 1621–1634.
[5] a) V. C. Ward, A. O. Chatzivasileiou, G. Stephanopoulos, *FEMS Microbiol. Lett.* **2018**, *365*, fny079; b) J. Grünler, J. Ericsson, G. Dallner, *Biochim. Biophys. Acta* **1994**, *1212*, 259–277.
[6] a) A. O. Chatzivasileiou, V. Ward, S. M. Edgar, G. Stephanopoulos, *Proc. Natl. Acad. Sci. USA* **2019**, *116*, 506–511; b) S. Lund, R. Hall, G. Williams, *ACS Synth. Biol.* **2019**, *8*, 232–238; c) M. A. Rinaldi, C. A. Ferraz, N. S. Scrutton, *Nat. Prod. Rep.* **2022**, *39*, 90–118; d) J. M. Clomburg, S. Qian, Z. Tan, S. Cheong, R. Gonzalez, *Proc. Natl. Acad. Sci. USA* **2019**, *116*, 12810–12815.
[7] a) A. Habenicht, J. Glomset, R. Ross, *J. Biol. Chem.* **1980**, *255*, 5134–5140; b) V. Quesney-Huneeus, M. H. Wiley, M. D. Siperstein, *Proc. Natl. Acad. Sci. USA* **1979**, *76*, 5056–5060; c) O. Kaneko, Y. Hazama-Shimada, A. Endo, *Eur. J. Biochem.* **1978**, *87*, 313–321.
[8] C. Schultz, M. Vajanaphanich, A. T. Harootunian, P. J. Sammak, K. Barrett, R. Y. Tsien, *J. Biol. Chem.* **1993**, *268*, 6316–6322.
[9] H. J. Jessen, T. Schulz, J. Balzarini, C. Meier, *Angew. Chem. Int. Ed.* **2008**, *47*, 8719–8722; *Angew. Chem.* **2008**, *120*, 8847–8850.
[10] C. Meier, *Antiviral Chem. Chemother.* **2017**, *25*, 69–82.
[11] a) C. M. Levinn, A. K. Steiger, M. D. Pluth, *ACS Chem. Biol.* **2019**, *14*, 170–175; b) K. G. Fosnacht, M. M. Cerda, E. J. Mullen, H. C. Pigg, M. D. Pluth, *ACS Chem. Biol.* **2022**, *17*, 331–339; c) J. Lou, M. L. Qualls, M. M. Hudson, D. P. McBee, J. A. Baccile, M. D. Best, *Chem. Eur. J.* **2022**, *28*, e202201057.
[12] a) L. Tian, Y. Yang, L. M. Wysocki, A. C. Arnold, A. Hu, B. Ravichandran, S. M. Sternson, L. L. Looger, L. D. Lavis, *Proc. Natl. Acad. Sci. USA* **2012**, *109*, 4756–4761; b) T. Gollnest, T. Dinis de Oliveira, A. Rath, I. Hauber, D. Schols, J. Balzarini, C. Meier, *Angew. Chem. Int. Ed.* **2016**, *55*, 5255–5258; *Angew. Chem.* **2016**, *128*, 5341–5344.

[13] a) A. Grumezescu, A. M. Holban, *The Science of Beverages*, Academic Press **2019**; b) A. Nakkarach, H. L. Foo, A. A.-L. Song, N. E. A. Mutalib, S. Nitisinprasert, U. Withayagiat, *Microbial. Cell. Factories* **2021**, *20*, 1–17; c) H. Mönkkönen, S. Auriola, P. Lehenkari, M. Kellinsalmi, I. E. Hassinen, J. Vepsäläinen, J. Mönkkönen, *Br. J. Pharmacol.* **2006**, *147*, 437–445; d) K. Ali, P. Mishra, A. Kumar, D. N. Reddy, S. Chowdhury, G. Panda, *Chem. Commun.* **2022**, *58*, 6160; e) K. W. George, M. G. Thompson, J. Kim, E. E. K. Baidoo, G. Wang, V. T. Benites, C. J. Petzold, L. J. G. Chan, S. Yilmaz, P. Turhanen, P. D. Adams, J. D. Keasling, T. S. Lee, *Metab. Eng.* **2018**, *47*, 60–72; f) L. J. Ruff, E. P. Brass, *Toxicol. Appl. Pharmacol.* **1991**, *110*, 295–302; g) R. Ebert, J. Meissner-Weigl, S. Zeck, J. Määttä, S. Auriola, S. Coimbra de Sousa, B. Mentrup, S. Graser, T. D. Rachner, L. C. Hofbauer, F. Jakob, *Mol. Cancer.* **2014**, *13*, 265.
[14] G. R. Fulmer, A. J. Miller, N. H. Sherden, G. E. Gottlieb, A. Nudelman, B. M. Stoltz, J. E. Bercaw, K. I. Goldberg, *Organometallics* **2010**, *29*, 2176–2179.

Manuscript received: September 5, 2022
Revised manuscript received: November 9, 2022
Accepted manuscript online: November 10, 2022
Version of record online: November 30, 2022